ISSN: 3064-6758 www.aristonpubs.com/sciengg-advances https://doi.org/10.69626/sea.2025.0026

RESEARCH ARTICLE

Impact of Ni Doping on the Structural, Optical, and Magnetic Properties of ZnO Thin Films Deposited via Chemical Bath Deposition

Gauri R. Patil [1,*], N. J. Kamble [1], B. P. Jamdade [1], Sikandar H. Tamboli [2]

ABSTRACT: Nickel-doped zinc oxide (Ni:ZnO) thin films were successfully synthesized on glass substrates using the chemical bath deposition (CBD) technique at 80°C. The structural, optical, and magnetic properties of the films were systematically analyzed using X-ray diffraction (XRD), scanning electron microscopy (SEM), ultraviolet-visible (UV-Vis) spectroscopy, and vibrating sample magnetometry (VSM). XRD patterns confirmed the formation of a hexagonal wurtzite structure in both undoped and Ni-doped ZnO samples, with no secondary phases detected, indicating successful incorporation of Ni ions into the ZnO lattice. SEM analysis revealed a variation in nanorod morphology with increasing Ni content, leading to a change in aspect ratio and surface roughness. UV-Vis spectroscopy showed a redshift in the absorption edge with increasing Ni concentration, suggesting band gap narrowing due to Ni-induced modifications in electronic states. Magnetic measurements confirmed room-temperature ferromagnetism in Ni-doped ZnO films, attributed to the exchange interactions between Ni ions and localized ZnO defects. The optimized 2% Ni-doped ZnO film exhibited enhanced structural and magnetic properties, making it a promising candidate for spintronic applications. This study provides valuable insights into the role of Ni doping in tailoring the multifunctional properties of ZnO thin films for optoelectronic and magnetic device applications.

Keywords: Ni-doped ZnO thin films, Chemical bath deposition, Optical band gap narrowing, Ferromagnetism.

Received: 29 July 2024; Revised: 21 September 2024; Accepted: 23 November 2024; Available Online: 09 December 2024

1. INTRODUCTION

Zinc oxide (ZnO), a wide-bandgap semiconductor material, has gained significant attention in recent years due to its unique combination of excellent optical, electrical, and magnetic properties, as well as its potential for applications in optoelectronics, photocatalysis, gas sensing, and spintronics [1, 2]. As an II-VI compound, ZnO naturally exhibits a hexagonal wurtzite structure and can be doped with various elements to tune its properties for specific applications. Among the various dopants, transition metals (TM), such as iron (Fe), cobalt (Co), and nickel (Ni), are particularly intriguing because of their ability to modify the electronic structure of ZnO and introduce magnetic characteristics [3, 4]. This class of materials, known as diluted magnetic semiconductors (DMSs), has garnered significant interest due to their potential for spintronic applications, where both the charge and spin of the carriers can be manipulated [5, 6].

Doped ZnO has shown promise in a variety of applications, including magnetic storage devices, spin-based transistors, and quantum computing, which require materials that exhibit both semiconducting and magnetic properties [7, 8]. In particular, Ni-doped ZnO has attracted considerable attention due to its potential for realizing ferromagnetism at room temperature, which is essential for future spintronic devices. The interaction between the doped Ni ions and the ZnO host lattice leads to localized magnetic moments, which

[1] Department of Physics, Dr. Patangrao Kadam Mahavidyalaya, Ramanadnagar (Burli), Shivaji University Kolhapur, MS, (416308) India.
[2] Shri Yashwantrao Patil Science College, Solankur, Shivaji University Kolhapur, MS, (416212) India.

*Author to whom correspondence should be addressed: patilgauri8888@gmail.com (Gauri R. Patil)

may give rise to ferromagnetic behavior [9, 10]. In this context, understanding how the concentration of Ni influences the structural, optical, and magnetic properties of ZnO thin films is crucial for the development of materials that can be utilized in spintronic applications [11].

The influence of Ni doping on ZnO has been studied through various deposition techniques, including sol-gel, hydrothermal, and chemical vapor deposition [12, 13]. Among these methods, the chemical bath deposition (CBD) technique has become increasingly popular due to its simplicity, low cost, and the ability to deposit films at relatively low temperatures [14, 15]. CBD allows for the controlled deposition of high-quality ZnO thin films on large substrates, making it an attractive method for scalable production. This technique has been successfully applied to synthesize Ni-doped ZnO films, where the doping concentration of Ni plays a crucial role in modifying the material's structural, optical, and magnetic properties [16, 17].

In the past decade, several studies have explored the impact of transition metal doping, especially Ni, on the properties of ZnO thin films [18, 19]. These studies have revealed that the concentration of Ni can significantly affect the structural orientation, grain size, and morphology of the films. For example, Ni doping has been shown to induce a shift in the X-ray diffraction (XRD) patterns of ZnO, altering the crystal structure and influencing the preferential orientation of the ZnO films [20, 21]. This change in the crystalline structure is often accompanied by variations in the optical band gap and the appearance of magnetic characteristics, which are essential for spintronic applications [22, 23].

One of the key findings in Ni-doped ZnO thin films is the change in the optical properties, specifically the absorption spectrum and the band gap. Doping with Ni leads to a redshift in the optical absorption edge, which can be attributed to the Burstein-Moss effect, where the conduction band is shifted to lower energies due to the introduction of Ni^{2+} ions into the ZnO lattice [24]. This results in a narrowing of the band gap, which can enhance the material's optical absorption, particularly in the ultraviolet (UV) region [25]. The reduction in band gap with increasing Ni concentration is an important factor that needs to be considered when designing ZnO-based devices for applications in optoelectronics and photovoltaics [26].

On the magnetic side, Ni doping has been shown to induce ferromagnetism in ZnO thin films, even though ZnO itself is non-magnetic [27]. This magnetic behavior arises from the interaction between the localized d-electrons of the Ni^{2+} ions and the conduction band electrons of ZnO [27]. The magnetic properties of Ni-doped ZnO can be influenced by several factors, including the concentration of Ni, the method of deposition, and the annealing conditions. Interestingly, studies have found that the magnetic properties of Ni-doped ZnO thin films are highly dependent on the doping concentration, with a certain concentration of Ni leading to enhanced ferromagnetism [27]. However, when the doping concentration exceeds a certain threshold, the magnetic properties tend to degrade, likely due to the formation of secondary phases or the weakening of the Ni-ZnO interaction [26].

The structural characteristics of Ni-doped ZnO thin films also play a critical role in determining the material's overall properties. The morphology of the films, such as the formation of nanorods or nanostructures, can significantly impact both the optical and magnetic behavior [27]. It has been observed that at lower Ni doping concentrations, ZnO thin films tend to form well-aligned nanorods, which provide a high surface area for interaction with light and enhance the material's optical properties. However, as the Ni concentration increases, the alignment of the nanorods becomes less uniform, and the films may become more disordered, which can reduce the overall quality of the material [25]. The size and shape of the nanorods, as well as the distribution of Ni within the ZnO matrix, are essential factors in tailoring the material's performance for specific applications [27].

In light of the significant role that Ni plays in modulating the properties of ZnO, several studies have focused on optimizing the synthesis conditions, such as the concentration of Ni, the deposition temperature, and the bath composition, to achieve the desired structural, optical, and magnetic properties [34]. The chemical bath deposition method, with its ability to produce large-area, uniform films at low temperatures, offers a promising route for the scalable production of Ni-doped ZnO thin films [24]. This study aims to investigate the effects of Ni doping on the structural, optical, and magnetic properties of ZnO thin films synthesized via the chemical bath deposition technique, with a focus on how varying Ni concentrations influence the material's characteristics. Through comprehensive analysis using X-ray diffraction (XRD), scanning electron microscopy (SEM), UV-Vis spectroscopy, and vibrating sample magnetometry (VSM), the study seeks to provide a deeper understanding of the fundamental changes induced by Ni doping in ZnO, paving the way for future spintronic and optoelectronic applications [25].

The goal of this research is to contribute to the growing body of knowledge on Ni-doped ZnO thin films and to provide insights into the relationship between Ni doping concentration and the resulting structural, optical, and magnetic properties. Such insights will be crucial for the development of ZnO-based materials with tailored properties for a range of advanced technological applications, particularly in the fields of spintronics, optoelectronics, and photocatalysis [26, 27].

2. EXPERIMENTAL DETAILS

In this study, the Ni-doped ZnO thin films were synthesized using the chemical bath deposition (CBD) method. This approach involves the deposition of thin films from a solution where the reactants are dissolved and subsequently react to form a solid phase that adheres to the substrate.

2.1. Preparation of Chemical Solution

Zinc nitrate dehydrate [$Zn(NO_3)_2 \cdot 2H_2O$] was used as the zinc source, and nickel nitrate [$Ni(NO_3)_2$] was used as the nickel source. For the synthesis of the Ni-doped ZnO thin films, 0.08 M zinc nitrate dehydrate was dissolved in deionized water to prepare the base solution. To achieve doping at different concentrations, nickel nitrate was added to the solution in various amounts, ranging from 1 atomic percent to 5 atomic percent. After the desired concentration of nickel nitrate was added, an aqueous ammonia solution was introduced to the mixture in order to adjust the pH of the solution to approximately 10.3, which is essential for the precipitation of ZnO. Initially, the solution became turbid due to the formation of ZnO nanoparticles, but this was resolved by the addition of excess ammonia to complete the precipitation process.

2.2. Substrate Preparation

The glass substrates were cleaned thoroughly to ensure a good-quality film deposition. Cleaning was carried out by placing the glass substrates in a sequence of acetone, isopropyl alcohol, and triply distilled water for 15 minutes each in an ultrasonic bath. After cleaning, the substrates were dried using high-pressure oxygen to remove any residual contaminants and moisture before further use in the deposition process.

2.3. Film Deposition

The cleaned glass substrates were immersed in the heated bath, which was maintained at a constant temperature of 80°C during the deposition process. The deposition time was set for 2 hours to allow for the precipitation of Ni-doped ZnO onto the substrates. The homogeneous precipitation resulted from the interaction of the zinc and nickel ions with the ammonia in the bath, leading to the formation of Ni-doped ZnO thin films. The thickness of the films was varied by controlling the deposition time and the concentration of the metal precursors in the solution.

2.4. Film Thickness Control

The film thickness was controlled by adjusting the deposition time in the chemical bath, which allowed for the formation of films of varying thicknesses. This parameter was optimized to achieve films that were suitable for further characterization and application in electronic devices.

3. RESULTS AND DISCUSSION

3.1. Structural Properties

XRD was used to examine the structural characteristics of undoped ZnO and Ni-doped ZnO thin films deposited via chemical bath deposition process; the findings for each sample are displayed in Figure 1. The XRD patterns of the samples are well with the JCPDS standard data of wurtzite (hexagonal) ZnO (No. 36-1451, a = 3.249 Å and c = 5.206 Å), undoped and Ni-doped ZnO samples showed peaks correspond to (100), (002), (101) and (102) planes. The (002) peak consistently displayed the highest intensity, suggesting that all the samples had a hexagonal crystal structure with a preferred orientation where the substrate normal was parallel to the ZnO (002) plane normal.

No diffraction peaks of other structures were detected in these samples, indicating that the Ni ion successfully occupied ZnO lattice site and there were no secondary phases or precipitates within the precision limit of XRD measurement. This is due to the presence of very low amount of Ni in the films as well as the presence of a very strong peak of (002) plane of ZnO dominating the XRD traces, which confirms that it is highly pure and single ZnO phase.

In line with earlier studies, it was shown that the synthesized undoped and Ni-doped ZnO exhibited preferential orientation along the (002) peak direction [15-17]. Since Zn^{2+} and Ni^{2+} have nearly identical ionic radii, the peak position remains unchanged with Ni doping, suggesting that Ni doping has no effect on the ZnO crystal [6], it also signifying that in the current composition region, metal ions (Ni) have a tendency to replace Zn sites without altering the crystal structure of ZnO (wurtzite structure) [6]. It may be inferred from the graph that the actual amount of Ni^{2+} doped into the ZnO crystal lattice may be related to the fact that the (002) diffraction peaks at 1% and 2% were higher than those of undoped ZnO, but the peaks at 3% were the same height (matched with JCPDS 78-0643). In 4% the height of (002) decreases than that of undoped ZnO, which is in good agreement with SEM results.

3.2. Surface Morphology and Compositional Properties

Figure 2 presents the SEM images of ZnO nanorods with varying Ni doping concentrations, revealing significant morphological changes induced by Ni incorporation. The nanorods exhibit a well-defined hexagonal prism shape, indicative of their preferential growth along the (002) crystallographic direction. However, distinct variations in nanorod alignment, diameter, and surface morphology are observed with increasing Ni doping. At a Ni doping concentration of 1% (Figure 2(b)), the nanorods display a relatively disordered arrangement compared to the undoped ZnO sample (Figure 2(a)). While some degree of vertical alignment is still visible, the nanorods do not exhibit complete uniformity, suggesting that the introduction of Ni begins to influence the nucleation and growth kinetics of ZnO. With an increase in Ni concentration to 2% (Figure 2(c)), the nanorods experience a noticeable increase in diameter, accompanied by the deposition of additional particles on the film surface. This suggests that Ni

incorporation promotes both lateral and vertical growth of ZnO nanorods, leading to the formation of a denser and more continuous film. The enhanced film quality at 2% Ni doping indicates an optimal balance between dopant incorporation and structural integrity. However, further increasing the Ni doping concentration to 3% and beyond (Figure 2(d, e)) results in significant irregularities in nanorod orientation, leading to a more disordered and non-homogeneous film structure. The excessive Ni incorporation disrupts the preferred (002) growth direction, causing a loss of vertical alignment and an increase in structural defects. These findings are consistent with X-ray diffraction (XRD) results, where a shift in the (002) peak position was observed as Ni content increased from 3% to 4%, indicating strain and lattice distortion within the ZnO crystal structure. It is important to note that the Ni doping concentrations used in this study remain well below the solid solubility limit of Ni in ZnO, ensuring that the observed morphological changes are not due to phase segregation but rather a direct result of Ni substitution within the ZnO lattice. These observations provide critical insights into the role of Ni doping in modulating the growth, alignment, and microstructure of ZnO nanorods, which are essential for optimizing their properties for optoelectronic and sensor applications. Energy dispersive X-ray spectroscopy (EDX) was employed to analyze the elemental composition of the Ni-doped ZnO thin films, ensuring the successful incorporation of Ni into the ZnO lattice (Figure 2(f)). EDX spectra were collected at multiple points across the film surface to confirm the presence of Zn, Ni, and O. The characteristic X-ray emission peaks corresponding to Zn (Lα, Kα), Ni (Kα, Lα), and O (Kα) were carefully analyzed to determine the elemental distribution and doping concentration. The uniform distribution of Ni within the ZnO matrix was validated through elemental mapping, which displayed a homogeneous dispersion of Ni without significant clustering or segregation. To quantify the Ni doping level, the atomic percentage of Ni in the films was calculated by comparing the relative intensity of Ni and Zn peaks. The analysis confirmed a systematic increase in Ni content with increasing doping concentration, indicating successful substitutional doping rather than phase separation or secondary phase formation. The absence of additional impurity peaks in the EDX spectra further affirmed the purity of the deposited films.

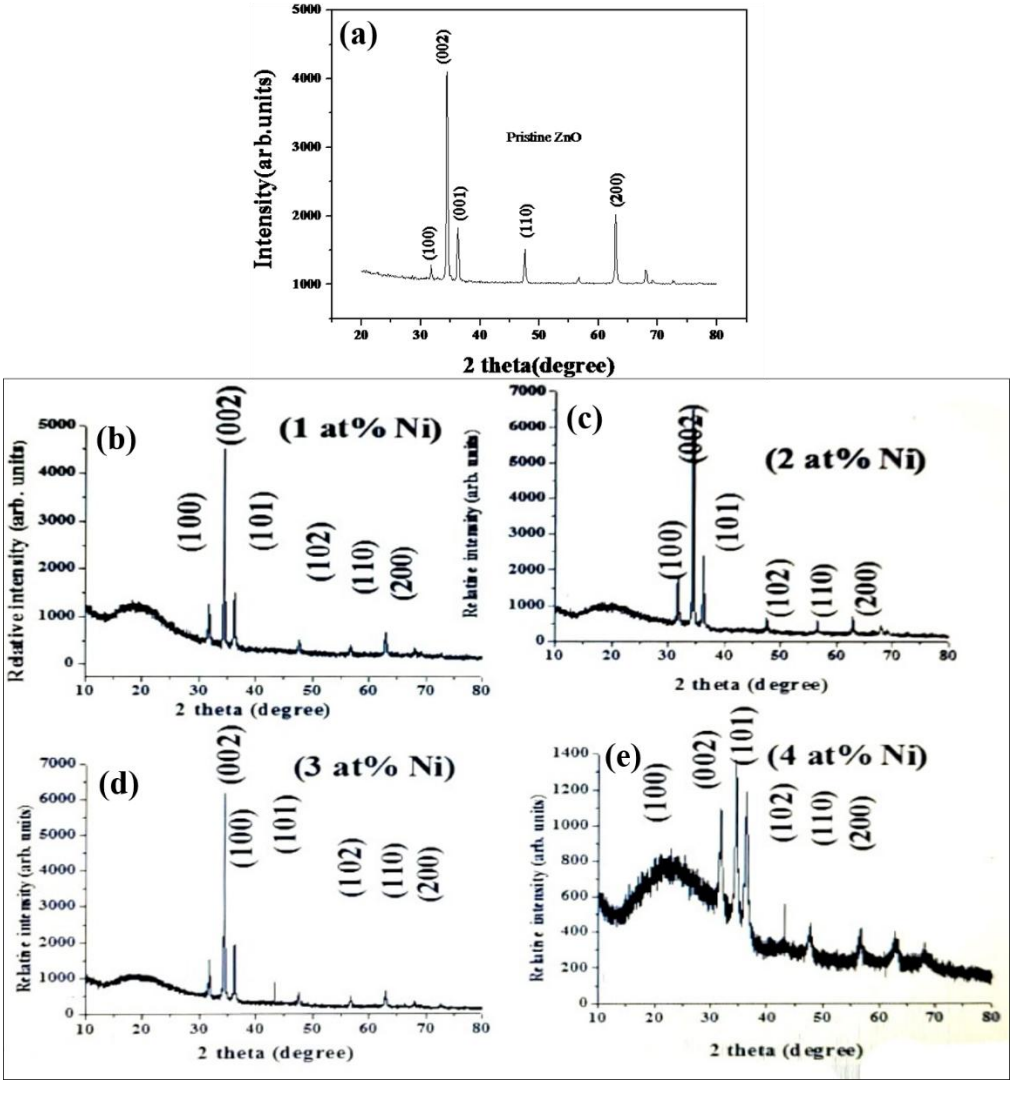

Fig. 1. XRD patterns of (a) pure ZnO and (b) 1%, (c) 2%, (d) 3%, and (e) 4 % Ni-doped ZnO thin films.

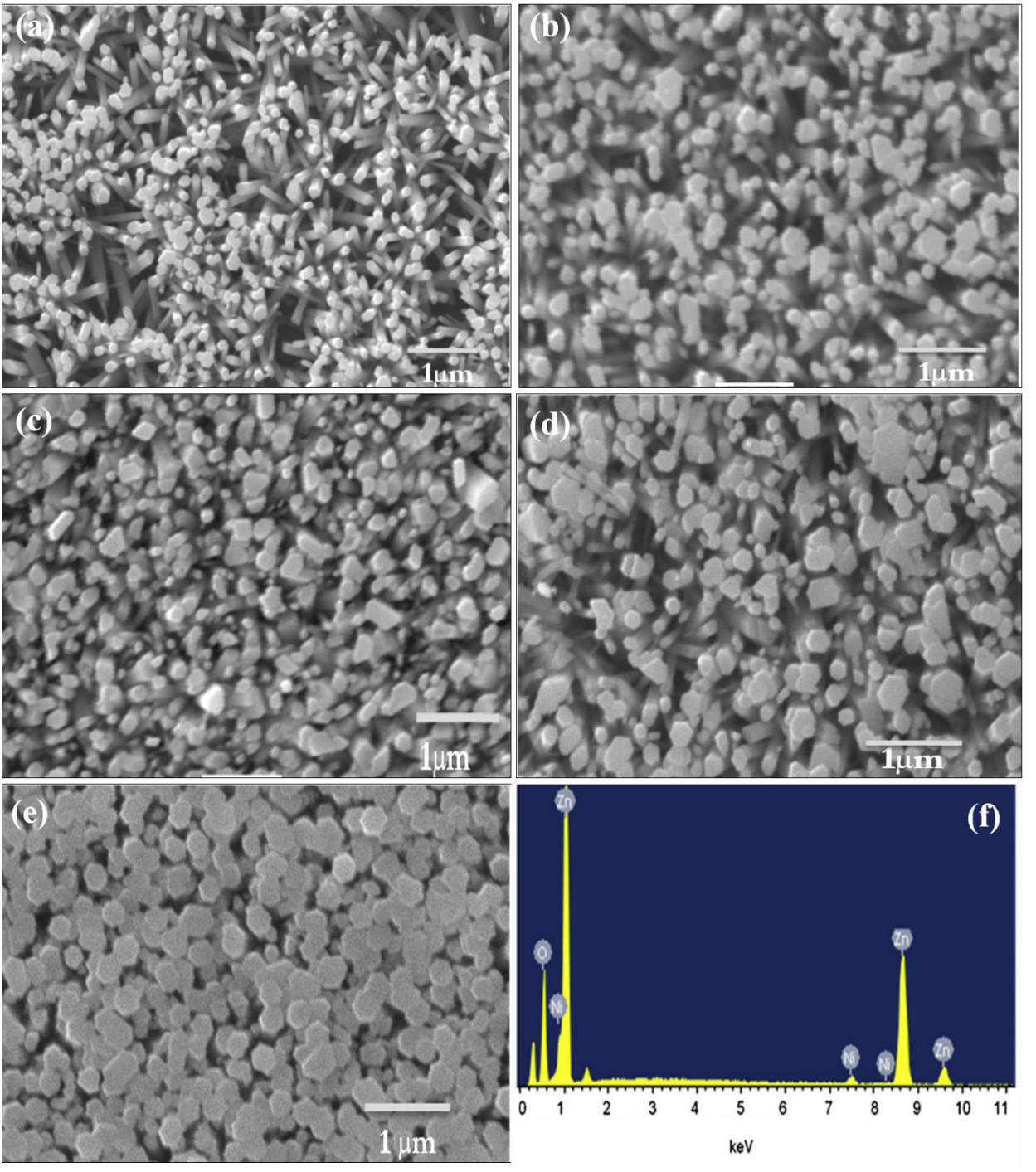

Fig. 2. SEM images of ZnO nanorods synthesized in reactive solutions with varying Ni doping concentrations: (a) Pristine ZnO, (b) 1% Ni-doped ZnO, (c) 2% Ni-doped ZnO, (d) 3% Ni-doped ZnO, (e) 4% Ni-doped ZnO. (f) EDX spectrum of 2% Ni-doped ZnO.

Figure 3 presents the TEM images of undoped ZnO and 2% Ni-doped ZnO thin films, highlighting the morphological and structural characteristics of the nanorods. The TEM images reveal that the ZnO nanorods exhibit a well-defined hexagonal shape with a smooth surface, and no observable clusters or agglomerations are present on the surface, indicating high crystallinity and uniformity of the synthesized structures. The structural consistency between the undoped and doped ZnO samples suggests that Ni incorporation does not significantly disrupt the ZnO nanorod formation process. Lattice spacing analysis provides further insight into the impact of Ni doping on the ZnO crystal structure. The measured interplanar spacing (d-spacing) of undoped ZnO is 0.26 nm, which is consistent with the (002)

plane of hexagonal ZnO, as reported in previous studies. Upon doping with 2% Ni, the d-spacing increases slightly to 0.265 nm for $ZnO_{0.95}Ni_{0.05}O$ nanorods. This expansion in lattice spacing can be attributed to the substitution of Zn^{2+} ions (ionic radius rZn^{2+}=0.60 Å with Ni^{2+} ions (ionic radius rNi^{2+}=0.69 Å), which possess a larger ionic radius. This substitution leads to a minor lattice distortion, causing an increase in the interplanar distance.

3.3. Optical Properties

The optical absorption behavior of undoped and Ni-doped ZnO nanorod arrays was examined using UV-visible spectroscopy, as shown in Figure 4(a). The absorption spectra reveal a distinct shift in the absorption edge with increasing Ni concentration, indicating modifications in the electronic structure of the ZnO lattice due to doping. A notable increase in the intensity of UV emission peaks is observed as the Ni concentration rises, highlighting the enhanced optical activity of the doped ZnO films. This enhancement suggests improved light absorption and possible alterations in carrier concentration.

To determine the optical band gap of the films, the Tauc plot method was employed, which is commonly used for direct bandgap semiconductors (Figure 4 (b)). The absorption coefficient (α) is related to the photon energy (hν) through the equation:

$$\alpha h\nu = A(h\nu - Eg)^{1/2} \quad (1)$$

where A is a constant, α\alphaα is the optical absorption coefficient, hν is the photon energy, and E_g represents the band gap energy. By extrapolating the linear region of the Tauc plot (αhν), the optical band gap values were estimated for the ZnO and Ni-doped ZnO thin films.

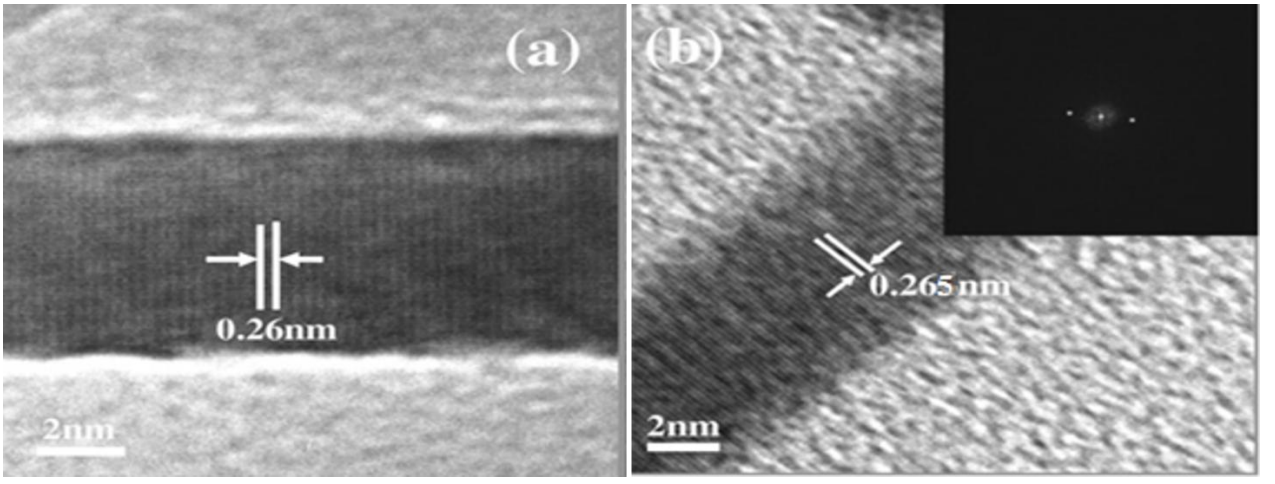

Fig. 3. HRTEM images of pristine ZnO and 2% Ni-doped ZnO thin films.

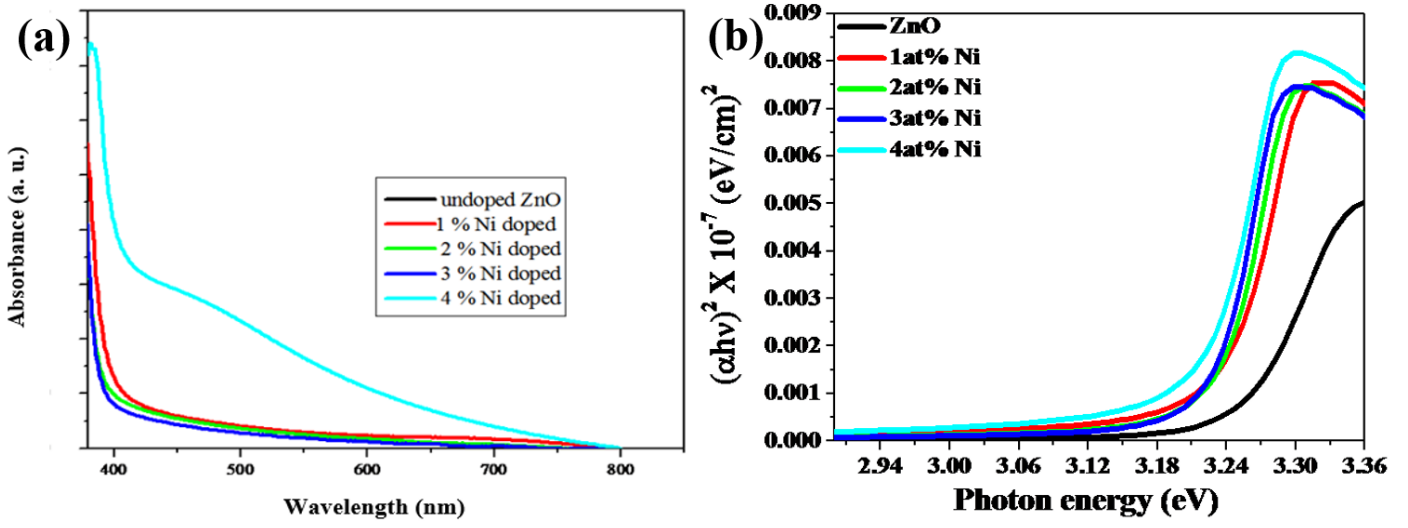

Fig. 4. (a) UV-visible absorption spectra of pristine and Ni-doped ZnO nanorod arrays. (b) Tauc plot for band gap estimation of undoped and Ni-doped ZnO thin films.

The results indicate that the band gap values varied from 3.17 eV to 3.25 eV, with a general trend of band gap reduction as the Ni doping concentration increased.

This decrease in band gap can be attributed to the Burstein-Moss effect, where the incorporation of Ni^{2+} ions into the ZnO lattice leads to an increase in carrier concentration, thereby shifting the Fermi level into the conduction band. The redshift of the absorption edge in Ni-doped samples further confirms the successful incorporation of Ni^{2+} ions within the ZnO matrix, influencing its electronic and optical properties.

3.4. Magnetic Properties

The magnetic properties of Ni-doped ZnO nanorods were investigated using magnetization vs. magnetic field (M–H) measurements, as shown in Figure 5. The M–H curves were recorded for undoped, 1%, 2%, 3%, and 4% Ni-doped ZnO thin films at room temperature, revealing distinct ferromagnetic characteristics in all samples.

For 1% Ni-doped ZnO, the remanent magnetization (M_m) and coercive field (Hc) were determined to be 0.25 emu/cm³ and 132 Oe, respectively. When the doping concentration increased to 2%, the values of M_m and Hc rose significantly to 0.38 emu/cm³ and 180 Oe, indicating an enhancement in ferromagnetic behavior. However, with a further increase in Ni concentration to 3%, both M_m and Hc decreased to 0.31 emu/cm³ and 78 Oe, respectively. This declining trend became even more pronounced in the 4% Ni-doped ZnO sample, where the M_m and Hc values dropped to 0.06 emu/cm³ and 123 Oe, respectively.

The observed enhancement in ferromagnetism from 1% to 2% Ni doping can be attributed to the higher incorporation of Ni^{2+} ions into the ZnO lattice, which contributes to a stronger exchange interaction. However, when the Ni doping level exceeds 3%, a significant reduction in ferromagnetism is observed. This decline can be explained by the limited solubility of Ni^{2+} in the ZnO lattice, which leads to the formation of non-magnetic or weakly magnetic defects. The results align well with the findings from UV–visible absorption spectra, XRD, and SEM analyses, confirming that only a fraction of Ni^{2+} ions successfully substitute Zn^{2+} in the host lattice, while excess Ni likely remains in interstitial positions or forms secondary phases that do not contribute to ferromagnetism.

There is ongoing debate regarding the origin of ferromagnetism in Ni-doped ZnO thin films. Some studies suggest that the ferromagnetism arises due to a homogeneous magnetic doping mechanism, while others propose that it results from magnetic precipitation [23–26]. Since Ni metal itself is a well-known ferromagnetic material, one possible explanation is that residual metallic Ni phases could contribute to the observed magnetization. However, in this study, the absence of detectable Ni secondary phases in XRD and SEM analyses suggests that the ferromagnetism does not originate from metallic Ni. The most plausible explanation for the observed ferromagnetism in Ni-doped ZnO thin films is the exchange interaction between free delocalized carriers (holes or electrons from the valence band) and the localized d-spins of Ni ions [6, 27]. This interaction, often referred to as a carrier-mediated exchange mechanism, is a key factor in determining the magnetic properties of diluted magnetic semiconductors (DMS). The observed changes in magnetization with increasing Ni content suggest that the ferromagnetic behavior is strongly dependent on the Ni concentration and its ability to effectively incorporate into the ZnO lattice without forming non-magnetic defects.

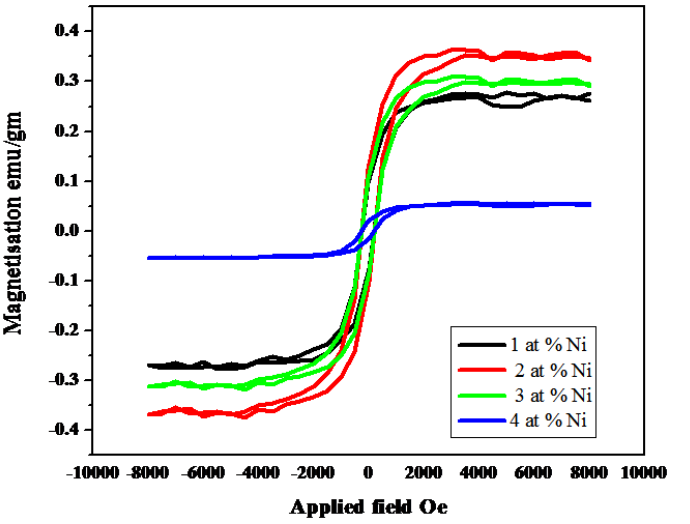

Fig. 5. Magnetization (M) vs. magnetic field (H) curves of undoped and Ni-doped ZnO thin films at room temperature.

4. CONCLUSION

This study highlights the significant impact of Ni doping on the structural, optical, and magnetic properties of ZnO thin films synthesized via the chemical bath deposition technique. XRD analysis confirmed that Ni-doped ZnO films retained the hexagonal wurtzite structure without any secondary phases, indicating the successful substitution of Ni^{2+} ions into the Zn^{2+} lattice sites. The peak intensity variations and broadening suggested minor lattice distortions induced by Ni doping. SEM analysis demonstrated a distinct morphological evolution, with an increase in nanorod diameter and surface roughness as Ni content increased. The optimized 2% Ni-doped ZnO film exhibited uniform nanorod growth, enhancing the overall film quality. Optical characterization via UV-Vis spectroscopy revealed a systematic redshift in the absorption edge with increasing Ni doping concentration, resulting in a reduced optical band gap. This band gap narrowing can be attributed to localized electronic states introduced by Ni doping, which alter the charge carrier dynamics in ZnO. Magnetic measurements further confirmed room-temperature ferromagnetism in Ni-doped ZnO films, likely due to exchange interactions between Ni^{2+} ions and native defects in the ZnO matrix. The emergence of ferromagnetic behavior, particularly in the 2% Ni-doped

sample, suggests its potential use in spintronic applications, where both optical and magnetic functionalities are essential. The Ni doping successfully modulated the structural, optical, and magnetic properties of ZnO thin films, making them suitable for a range of advanced applications, including optoelectronics, spintronics, and magnetic sensing devices. Future research should focus on optimizing the synthesis conditions and exploring the effects of alternative dopants to further enhance the multifunctionality of ZnO-based materials.

DECLARATIONS

Ethical Approval

We affirm that this manuscript is an original work, has not been previously published, and is not currently under consideration for publication in any other journal or conference proceedings. All authors have reviewed and approved the manuscript, and the order of authorship has been mutually agreed upon.

Funding

Not applicable

Availability of data and material

All of the data obtained or analyzed during this study is included in the report that was submitted.

Conflicts of Interest

The authors declare that they have no financial or personal interests that could have influenced the research and findings presented in this paper. The authors alone are responsible for the content and writing of this article.

Authors' contributions

All authors contributed equally in the preparation of this manuscript.

ACKNOWLEDGEMENTS

Gauri R. Patil is thankful to Shivaji University, Kolhapur for providing financial assistance under Diamond Jubilee Research Initiation Scheme 2024-25.

REFERENCES

[1] Zaouche, C., Dahbi L. and Benramache S., **2023**. Study the effect of Ni doping on structural, optical and electrical properties of Zn1-xNixO thin films deposited by spray pyrolysis technique". *Journal Of Ovonic Research* 19, pp 197-205. https://doi.org/10.15251/JOR.2023.192.197.

[2] Wolf, S. A., Awschalom, D.D., Buhrman, R.A., Daughton, J.M., Von Molnar, S., Roukes, M.L., Chtchelkanova, A.Y. and Treger, D.M., **2001**. Spintronics: A Spin-Based Electronics Vision for the Future. *Science* 294, pp 1488. DOI: 10.1126/science.1065389.

[3] Prokes, M. and Wang, K.L., **1999**. Novel Methods of Nanoscale Wire Formation. *MRS Bulletin.* 24, pp 13-20. https://doi.org/10.1557/S0883769400052842.

[4] Hu, J., Odom, T.W. and Lieber, C.M., **1999**. Chemistry and physics in one dimension: Synthesis and properties of nanowires and nanotubes. *Accounts of Chemical Research* 32, pp 435. https://doi.org/10.1021/ar9700365.

[5] Meng, S., Li, D., Zheng, X., Wang, J., Chen, J., Fang, J., Shao, Y. and Fua, X., **2013**. ZnO photonic crystals with enhanced photocatalytic activity and photostability. *Journal of Materials Chemistry A,* 1, pp 2744. https://doi.org/10.1039/C2TA01327D.

[6] Cheng, C., Xu, G.Y., Zhang, H.Q. and Luo, Y., **2008**. Hydrothermal synthesis Ni-doped ZnO nanorods with room-temperature ferromagnetism. *Materials Letters* 62, pp 1617-1620. https://doi.org/10.1016/j.matlet.2007.09.035.

[7] Sugihartono, I., Aliffah, F. N., Putri, P. L., Manawan, M., Isnaeni, I. and Tan, S. T., **2023**. The role of Ni-Doped ZnO thin films on Methylene Blue (MB) photodegradation under visible irradiation. *Journal of Physics: Conference Series,* 2596, pp 012012. **DOI** 10.1088/1742-6596/2596/1/012012.

[8] Anandan M., Dinesh S., Christopher B., Krishnakumar N., Krishnamurthy b., and Ayyar M. **2024**. Multifaceted investigations of co-precipitated Ni-doped ZnO nanoparticles: Systematic study on structural integrity, optical interplay and photocatalytic performances. *Physica B: Condensed Matter* 674, pp 415597. https://doi.org/10.1016/j.physb.2023.415597.

[9] Elilarassi, R., and Chandrasekaran G., **2010**. Structural, optical and magnetic properties of nanoparticles of ZnO:Ni—DMS prepared by sol–gel method. *Materials Chemistry and Physics.* 123, pp 450-455. https://doi.org/10.1016/j.matchemphys.2010.04.039.

[10] Xia C., Hu C., Tian Y., Wan B., Xu J., and He X., **2010**. Room-temperature ferromagnetic properties of Ni-doped ZnO rod arrays. *Physica E: Low-dimensional Systems and Nanostructures* 42, pp 2086-2090. https://doi.org/10.1016/j.physe.2010.04.003.

[11] Wu, D., Yang, M., Huang, Z., Yin, G., Liao, X., Kang, Y., Chen, X., and Wang, H., **2009**. Preparation and properties of Ni-doped ZnO rod arrays from aqueous solution. *Journal of Colloid Interface Science* 330, pp 380-385. https://doi.org/10.1016/j.jcis.2008.10.067.

[12] Abed, S., Aida, M.S., Bouchouit, K., Arbaoui, A.,

Iliopoulos, K., and Sahraoui, B. **2011**. Non-linear optical and electrical properties of ZnO doped Ni Thin Films obtained using spray ultrasonic technique. *Optical Materials* 33, 968-972. https://doi.org/10.1016/j.optmat.2011.01.018.

[13] Lupan, O., Pauporte, T. and Viana, B., **2010**. Low-Temperature Growth of ZnO Nanowire Arrays on p-Silicon (111) for Visible-Light-Emitting Diode Fabrication, *Journal of Physical Chemistry C* 114, pp 14781-14785. https://doi.org/10.1021/jp104684m.

[14] Balti, I., Mezni, A., Dakhlaoui-Omrani, A., Léone, P., Viana, B., Brinza, O., Smiri, L., and Jouini N., **2011**. Comparative Study of Ni- and Co-Substituted ZnO Nanoparticles: Synthesis, Optical, and Magnetic Properties *Journal of Physical Chemistry C* 115, pp 15758-15766. https://doi.org/10.1021/jp201916z.

[15] Kim, T.K., Kim, G. H., Woo, J. C. and Kim, C. **2008**. Characteristics of Nickel-doped Zinc Oxide thin films prepared by sol–gel method, *Surface and Coatings Technology* 202, pp 5650-5653. https://doi.org/10.1016/j.surfcoat.2008.06.078.

[16] Gayen, R.N., Rajaram, A., Bhar, R. and Pal A.K. **2010**. Ni-doped vertically aligned zinc oxide nanorods prepared by hybrid wet chemical route. *Thin Solid Films* 518, pp 1627-1636. https://doi.org/10.1016/j.tsf.2009.11.067.

[17] Iskenderoğlu, D. and Guney, H., **2017**. Synthesis and characterization of ZnO:Ni thin films grown by spray-deposition. *Ceramics International* 43, pp 16593-16599. https://doi.org/10.1016/j.ceramint.2017.09.047.

[18] Pearton, S.J., Heo, W.H., Ivill, M., Norton, D.P. and Steiner, T. **2004**. Dilute magnetic semiconducting oxides, *Semiconductor Science and Technology* 19, pp R59. https://dx.doi.org/10.1088/0268-1242/19/10/R01.

[19] Zaman, Y., Ishaque, M.Z., Waris, K., Shahzad, M., Siddique, A. B., Arshad, M. I., Zaman, H., Ali, H. M, Kanwal, F., Aslam, M. and Mustaqeem, M. **2023**. Modified physical properties of Ni doped ZnO NPs as potential photocatalyst and antibacterial agents. *Arabian Journal of Chemistry* 16, pp105230. https://doi.org/10.1016/j.arabjc.2023.105230.

[20] Burstein, E. **1954**. Anomalous Optical Absorption Limit in InSb, *Physical Review B* 93, pp 632. https://doi.org/10.1103/PhysRev.93.632.

[21] Pawar, B.N., Jadkar, S.R. and Takwale, M.G. **2005**. Deposition and characterization of transparent and conductive sprayed ZnO:B thin films, *Journal of Physics and Chemistry of Solids*, 66, pp 1779-1782. https://doi.org/10.1016/j.jpcs.2005.08.086.

[22] Eppakayala, J., Mettu, M. R., Pendyala, V. R. and Madireddy J. R., **2020**. Synthesis, structural and optical properties of Ni doped ZnO nanoparticle – A chemical approach, *Materials Today: Proceeding* 26, pp 148-153. https://doi.org/10.1016/j.matpr.2019.08.099.

[23] Park, J.H., Jang, M.G. and Ryu, S. **2004**, Co-Metal Clustering as the Origin of Ferromagnetism in Co-Doped ZnO Thin Films, *Applied Physics Letters* 84, pp 1338. https://doi.org/10.1063/1.1650915.

[24] Kim, Y.M., Yoon, M., Park, I.-W., Park, Y.J. and Lyou, J. H., **2004**. Synthesis and magnetic properties of $Zn_{1-x}Mn_xO$ films prepared by the sol–gel method, *Solid State Communications* 129, pp175-178. https://doi.org/10.1016/j.ssc.2003.09.035.

[25] Sharma, P., Gupta, A., Rao, K.V., Owens, F.J., Sharma, R., Ahuja, R., Osorio Guillen, J.M., Johansson, B. and Gehring, G.A. **2003**. Ferromagnetism above room temperature in bulk and transparent thin films of Mn-doped ZnO, *Nature Materials* 2, pp673-677. https://doi.org/10.1038/nmat984.

[26] Sharma, P., Gupta, A., Owens, F.J., Inoue, A. and Rao, K.V., **2004**. Room temperature spintronic material—Mn-doped ZnO revisited. *Journal of Magnetism and Magnetic Materials* 282, pp115-121. https://doi.org/10.1016/j.jmmm.2004.04.028.

[27] Kittilstved, K.R., Liu, W.K. and Gamelin, D.R., **2006**. Electronic structure origins of polarity-dependent high-TC ferromagnetism in oxide-diluted magnetic semiconductors, *Nature Materials* 5, pp291-297. https://doi.org/10.1038/nmat1616.